TOMOGRAPHY® RESEARCH ARTICLE

Assessing Mucosal Inflammation in a DSS-Induced Colitis Mouse Model by MR Colonography

Inbal E. Biton[1], Noa Stettner[1,2,3], Ori Brener[1], Ayelet Erez[2], Alon Harmelin[1], and Joel R. Garbow[4]

[1]Department of Veterinary Resources, Weizmann Institute of Science, Rehovot, Israel; [2]Department of Biological Regulation, Weizmann Institute of Science, Rehovot, Israel; [3]Koret School of Veterinary Medicine, Hebrew University, Rehovot, Israel; and [4]Biomedical Magnetic Resonance Laboratory, Mallinckrodt Institute of Radiology, Washington University, St. Louis, MO

Corresponding Author:
Joel R. Garbow, PhD
Biomedical Magnetic Resonance Laboratory, Mallinckrodt Institute of Radiology, Campus Box 8227, 4525 Scott Avenue, Washington University, St. Louis, MO, 63110;
E-mail: garbow@wustl.edu

Key Words: magnetic resonance imaging, MR colonography, T2 map, inflammatory bowel disease, ulcerative colitis

Abbreviations: Inflammatory bowel disease (IBD), magnetic resonance imaging (MRI), ulcerative colitis (UC), Crohn's disease (CD), computed tomography (CT), T2-weighted (T2W), magnetic resonance (MR), dextran sodium sulfate (DSS), hematoxylin and eosin (H&E)

ABSTRACT

Inflammatory bowel disease (IBD) is characterized by a chronic flaring inflammation of the gastrointestinal tract. To determine disease activity, the inflammatory state of the colon should be assessed. Endoscopy in patients with IBD aids visualization of mucosal inflammation. However, because the mucosa is fragile, there is a significant risk of perforation. In addition, the technique is based on grading of the entire colon, which is highly operator-dependent. An improved, noninvasive, objective magnetic resonance imaging (MRI) technique will effectively assess pathologies in the small intestinal mucosa, more specifically, along the colon, and the bowel wall and surrounding structures. Here, dextran sodium sulfate polymer induced acute colitis in mice that was subsequently characterized by multisection magnetic resonance colonography. This study aimed to develop a noninvasive, objective, quantitative MRI technique for detecting mucosal inflammation in a dextran sodium sulfate–induced colitis mouse model. MRI results were correlated with endoscopic and histopathological evaluations.

INTRODUCTION

Inflammatory bowel disease (IBD) encompasses 2 major forms of intestinal inflammation—ulcerative colitis (UC) and Crohn's disease (CD)—both of which are characterized by chronic exacerbations of inflammation in the gastrointestinal tract (1). IBD is a global disease of increasing prevalence. More than 1 million individuals in the USA and 2.5 million in Europe are estimated to have IBD, with annual health-care costs of $6 billion and €4.6–5.6 billion, respectively (2, 3). Patients with IBD experience clinical gastrointestinal indications, as well as chronic emotional symptoms, that can severely reduce quality of life and ability to work. Imaging techniques can play a key role in the diagnosis and lifelong evaluation of patients with IBD. In particular, the development of noninvasive imaging techniques that can perform the initial screening and diagnosis of IBD, in particular, at early stages, will be of considerable value.

The clinical severity of IBD is usually proportional to the extent of bowel involved and the intensity of the inflammation process in the affected tissue (4). The inflammation in CD may potentially extend to any part of the gastrointestinal tract, whereas inflammation in UC extends from the rectum and involves the distal part of the colon (5). The inflammatory process in UC is typically confined to the innermost lining or mucosa and may involve all of the gastrointestinal tract continuously, whereas the inflammatory process in CD may involve all layers of the intestine, but a "skip lesion" appears between the healthy and affected tissue (6). The etiology of both diseases remains unclear, although a combination of genetic, environmental, and immunological factors contributes to disease initiation and progression (7).

IBD is, in general, diagnosed on the basis of a combination of clinical, pathological, radiological, endoscopic, and laboratory indications (8). To determined disease activity and tailor IBD therapy, the inflammatory state of the colon should be assessed. However, clinical features alone are neither sensitive nor specific enough for grading lesion severity in IBD, and imaging plays a key role in its diagnosis (9, 10). Endoscopy is the gold-standard technique for diagnosis of IBD, aiding direct visualization of the colonic mucosa, the target of the disease. Endoscopy helps to identify inflammation, including its location and severity, and obtain biopsies needed to confirm the diagnosis. However, endoscopy is an invasive technique that requires patient preparation and discomfort, and interpretation of its results is highly operator/radiologist-dependent (11, 12). Therefore, alter-

ISSN 2379-1381 http://dx.doi.org/10.18383/j.tom.2017.00021

native, noninvasive imaging modalities are being explored to complement endoscopy for diagnosis of IBD. Computed tomography (CT) can be used to diagnose and evaluate the extent and severity of inflammatory diseases in the small bowel and colon. However, owing to the radiation exposure associated with CT, it is not a useful imaging technique for multiple follow-up examinations after therapy, particularly in young patients (11). Also, CT suffers from low diagnostic sensitivity for the early stages of UC (8).

Recently, magnetic resonance imaging (MRI) has emerged as an important imaging modality for detecting morphologic changes and inflammatory activity associated with IBD in both patients (11, 13–17) and animal models (8, 9, 18–21). MRI is a noninvasive technique, using nonionizing radiation, which has equal or better sensitivity than CT for imaging IBD (11). A significant advantage of MRI is the existence of multiple, intrinsic contrast mechanisms that may be used to highlight intestinal tissues with inflammation. In contrast-enhanced, T1-weighted images, the degree of gadolinium enhancement at the level of the colon wall correlates qualitatively with disease activity (8, 15, 16). In a complementary manner, T2-weighted (T2W) sequences highlight tissue–fluid content, and are, therefore, sensitive to inflammation and thickening of the colon wall. However, these findings are consistently observed in only severe and active UC. In moderate and quiescent stages of UC, no effect on the colon wall thickness is found (15), and current MRI methods are not sensitive enough for robust detection of these stages of UC. The development of robust, noninvasive imaging protocols that can be performed repetitively to detect mucosal inflammation and score the extent and severity of disease, in particular at early stages, will be important for IBD diagnosis and therapy.

The most commonly used animal models of IBD involve chemically induced intestinal inflammation. Such models, which are straightforward and generate a nearly immediate onset of inflammation, display many important immunological and histopathological characteristics of IBDs seen in humans (6, 7). For example, introducing dextran sodium sulfate (DSS) (≥2.5% wt/vol) in drinking water for several days induces acute colitis in mice, characterized by a variety of symptoms that are consistent with colitis in patients, including, hyperemia, ulcerations, moderate-to-severe submucosal edema, and lesions, accompanied by histopathological changes that include infiltration of granulocytes, which are manifested in the form of bloody diarrhea (4). It is generally believed that DSS is directly toxic to gut epithelial cells of the basal crypts and affects the integrity of the mucosal barrier (6, 7). Because of this direct toxicity, DSS causes erosions, with complete loss of surface epithelium, and deformity in the epithelial integrity, thereby increasing colonic mucosal permeability. DSS-induced UC appears to be more severe in the distal colon, although it causes an increase in the production of all proinflammatory cytokines in both midcolon and distal colon (4).

Several groups have described magnetic resonance (MR) studies of DSS-treated mice. Melgar et al., established a rapid MRI screening tool, based upon colon wall thickness and hyperintensity in T2W images, for distinguishing between healthy and DSS-treated mice (20). Using T1-weighted imaging and an iron oxide-based ink solution, Walldorf et al., measured colon wall thickness and were able to discriminate between healthy control mice, DSS-colitis mice, and DSS-colitis mice treated with an anti-inflammatory (21). In studies using T2W images and maps, Breynaert et al., investigated bowel wall inflammation and fibrosis in a murine model of IBD, with repeated cycles of DSS (1.5%–2% wt/vol) designed to mimic the relapsing nature of the disease (19). In the PG-PS rat model, Alder et al., showed that magnetization transfer MRI could differentiate fibrotic from inflamed bowel (18). Although these MR studies demonstrated success in distinguishing healthy from damaged, inflamed colon, none displayed the sensitivity required for early-stage detection and grading of IBD.

The aim of this study was to develop an improved, noninvasive, in vivo MRI-based grading tool for quantifying IBD, on a positional basis along the length of the colon, in a DSS-induced murine model of colitis. We correlated MRI-derived metrics, based on colon wall thickness and T2 maps of colon tissue, with endoscopic and histological features, in both normal colons and DSS-treated colons. We also estimated the sensitivity of this new MRI-based grading tool at different positions within the colon, which will be important for early-stage diagnosis of IBD.

METHODOLOGY

Animals

Animal experiments were approved by the Weizmann Institute Animal Care and Use Committee following Israeli, US National Institutes of Health, and European Commission guidelines. Eight-week-old male C57BL/6 mice (n = 26) were obtained from Envigo (Rehovot, Israel). Mice were treated with 0%–2% (wt/vol) DSS (MP Biomedicals; molecular weight, 36,000–50,000 Da) in drinking water for 7 days, followed by 5 days of regular water (7). The mice were divided into the following 5 groups: untreated (n = 6), 0.5% DSS (n = 5), 1% DSS (n = 5), 1.5% DSS (n = 5), and 2% DSS (n = 5) treated mice. Survival and changes in body weight of the animals were monitored daily over the course of colitis development. Mice were monitored throughout the experiment, and any that showed extreme distress, became moribund, or lost more than 20% of initial body weight were euthanized.

MRI

All mice were imaged on days 7 and 11 post DSS treatment. Prior to imaging, animals were anesthetized using intramuscular injection of a mix of Domitor (Medetomidine, 1 mg/kg; Orion Corporation, Espoo, Finland) and Ketamine (75 mg/kg; Vetoquinol, Lure, France) and were administered successive warm saline enemas (~2 mL) to clear the colon of solid fecal material. Two milliliters of perfluorinated oil (Fomblin Y LVAC 06/6 perfluoropolyether oil; Sigma-Aldrich, St. Louis, MO) were introduced into the colon via a rectal catheter consisting of microbore tubing (20G cannula, Delta Med). The setup of the mice in the MRI animal holder is shown in Figure 1A. At the end of the MRI protocol, the anesthetized mice were injected intraperitoneally with Antisedan (1 mg/kg; Orion Corporation).

MRI experiments were performed on 9.4 Tesla BioSpec Magnet 94/20 USR system (Bruker BioSpin Corporation, Billerica, MA) equipped with a gradient coil system capable of producing pulsed gradients of up to 40 G/cm in each of 3 orthogonal directions. MR images were acquired using a quadrature volume coil with 35-mm inner diameter (Bruker). The T2 maps

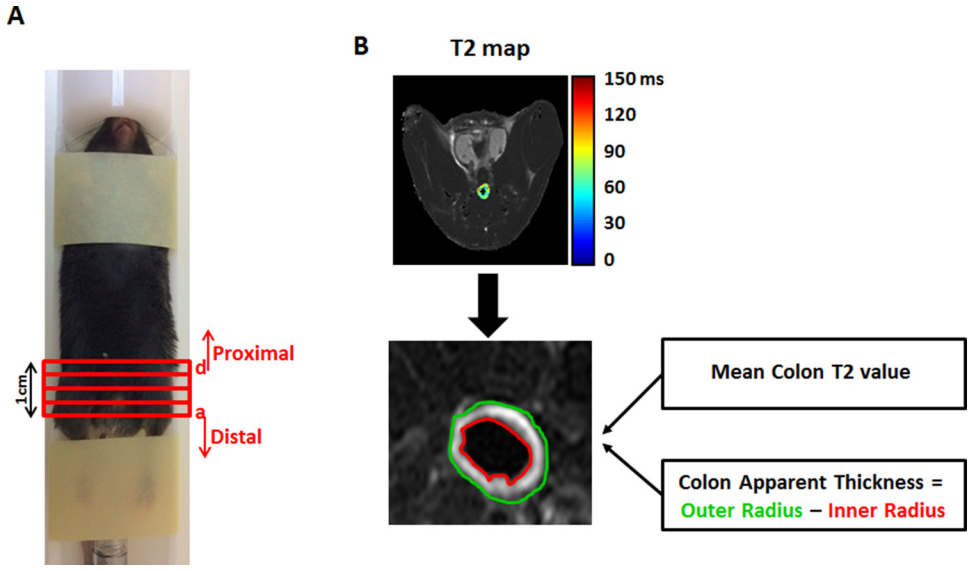

Figure 1. In vivo mouse magnetic resonance imaging (MRI) colonoscopy experiment. Mice were set up in a dedicated MRI animal holder (A). The length of the scanned colon was ~1 cm. Histological sections were taken from 4 regions [in red, sections (a)–(d)] of this area. The most distal portion of the colon is defined as (a) and the most proximal portion as (d). T2 maps of the colon, calculated on a pixel-by-pixel basis, with selection of two regions of interest, yellow and red, representing the outer and inner colon radii, respectively (B). Mean T2 value and apparent thickness were calculated for each section of the colon.

were acquired using multisection spin-echo imaging, with interleaved sections and the following parameters: a repetition delay of 3000 milliseconds, 16 time echo increments (linearly from 10 to 160 milliseconds), matrix dimension of 256 × 128 (interpolated to 256 × 256) and 2 averages, corresponding to an image acquisition time of 12 minutes 48 seconds. Fourteen contiguous, 1-mm-thick sections, were acquired, with a field of view of 3.0 × 2.5 cm^2.

Endoscopy

Colonoscopy was performed on days 7 and 11 post DSS treatment to monitor the severity of colitis. Colitis was scored by a single rater according to the Murine Endoscopic Index of Colitis Severity (MEICS), considering five factors: (i) thickening of the colon wall; (ii) changes in vascular pattern; (iii) presence of fibrin; (iv) mucosal granularity; and (v) stool consistency. Each factor was scored with a value between 0 and 3. The cumulative score ranged from 0 (no signs of inflammation) to 15 (signs of very severe inflammation) (22). Healthy mice typically have cumulative scores of 0–3.

Histopathology

On the day of sacrifice (day 11), the colons were removed and their lengths measured. They were then fixed in 2.5% paraformaldehyde solution overnight at 4°C, embedded in paraffin, sectioned, and stained with hematoxylin and eosin (H&E). H&E-stained tissue was examined in a blinded manner by a gastrointestinal pathologist. Tissues were graded on a 0–4 scale based on the parameters of inflammation severity (7), according to the following scoring system: 0, no evidence of inflammation; 1, low level of inflammation with scattered infiltrating mononuclear cells, 1–2 foci; 2, moderate inflammation with multiple foci; 3, high level of inflammation with increased vascular density and marked wall thickening; and 4, maximal severity of inflammation with transmural leukocyte infiltration and loss of goblet cells.

Image Analysis

All image analyses were performed using purpose-written MATLAB (R2013B) scripts. Quantitative T2 maps were generated from multiecho, T2W images by fitting the multiecho signal as a monoexponential decay. Colon walls were manually segmented as hyperintense (compared with muscle tissue) regions in T2W spin-echo images. T2 maps of the colon were calculated on a pixel-by-pixel basis and overlaid on T2W images. Two regions of interest were drawn on each map, representing the inner (red) and outer (yellow) radii of the colon (Figure 1B). In performing this analysis, we assumed that the colon is circular in shape, and we extracted its radius as the difference between the areas of the outer and inner circles. Two parameters, the mean T2 value of the colon, and the colon apparent thickness, were calculated for each section. Results are presented on a section-by-section basis and as average values across all sections.

Statistical Methods

The results are reported as mean ± SD. Student *t* test was used to compare means of 2 groups, with $P < .05$ defining statistical significance.

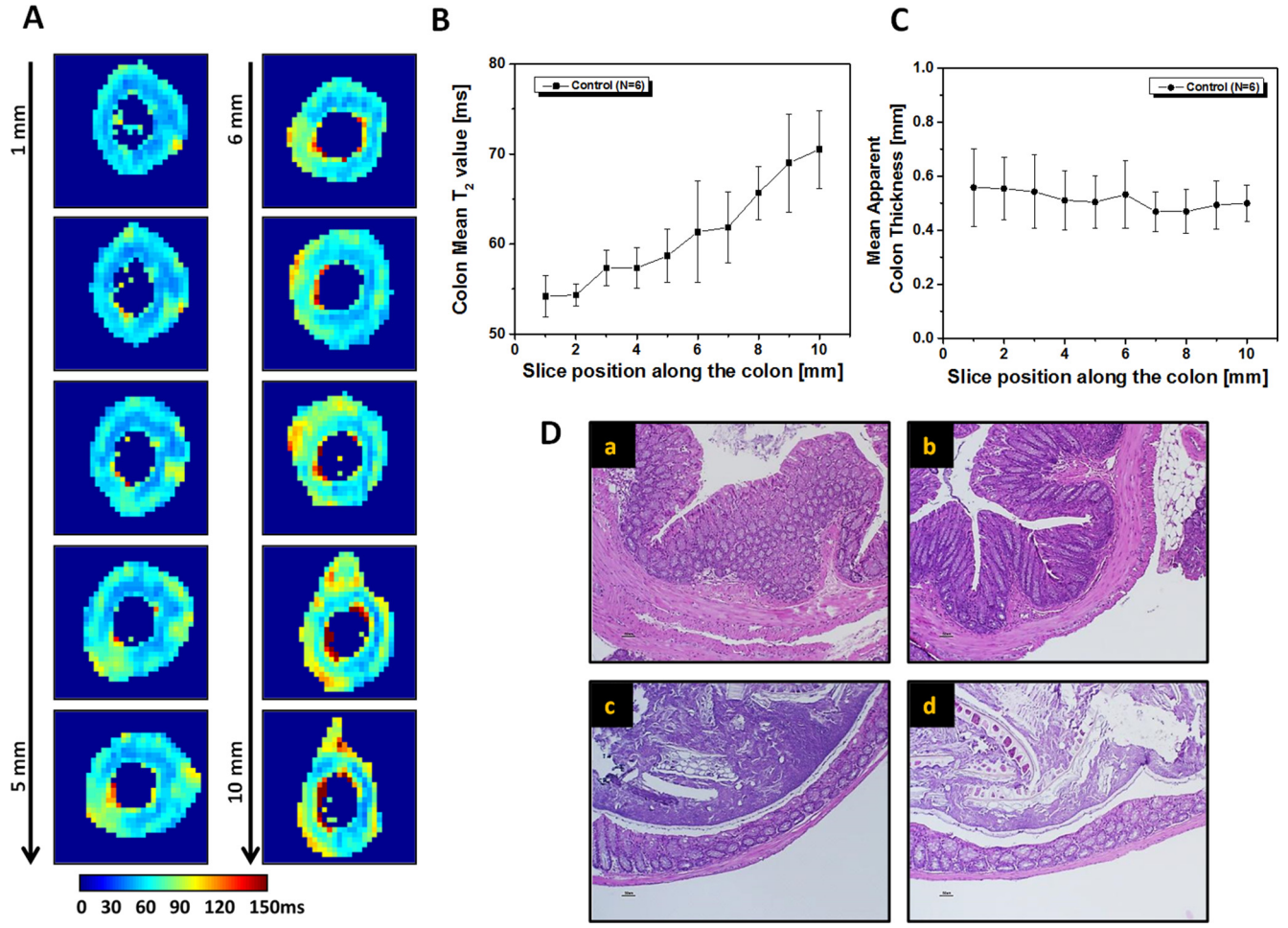

Figure 2. In vivo MRI colonoscopy of untreated mouse. T2 maps of representative, untreated colon at different sections along the colon (A). The most distal part is labeled as 1 and the most proximal as 10. Colon wall mean T2 values (B) and mean apparent thickness (C) as functions of section position along the colon are presented. Values are reported as mean ± SD. Hematoxylin and eosin (H&E)-stained transverse sections of control colon obtained from 4 different points (a–d) along the imaging area (~1 cm) (D). The most distal part is shown in (a) and the most proximal part in (d).

RESULTS

In Vivo MRI Colonoscopy of Untreated Mice

Multisection MR images were collected in a cohort of untreated control mice, and revealed clear differences along the length of the colon in these animals. T2 maps, shown in Figure 2A, illustrate a trend of increasing T2, from distal to proximal end, along the measured region of the colon. Quantitative measurement of T2 values of the colon wall, plotted in Figure 2B, shows significantly higher values in proximal vs distal regions (71 ± 1 milliseconds for the most proximal image section vs 54 ± 1 milliseconds for the most distal section). However, as shown in Figure 2C, no significant differences were observed in mean colon wall thickness along the length of the colon (0.50 ± 0.07 mm for the most proximal image section vs 0.56 ± 0.14 mm for the most distal section).

Histological examination of untreated colon at 4 different points along the measured colon confirmed the MRI colonoscopic observation (Figure 2D). There were no signs of inflammation or crypt damage and no variation in the thickness of the colonic wall. Nonetheless, microscopic examination of the colon at 4 different points along its length showed differences in tissue architecture, consistent with the positional-dependent T2 values measured in the MRI colonoscopy experiment. The thickness of the muscular layer, in particular that of the circular layer, decreases from distal to proximal (23). The diameter of the colon is also dependent on the presence or absence of fecal pellets [present in (c) and (d), but not in (a) or (b)].

In Vivo MRI Colonoscopy of 1% DSS-Induced Acute Colitis

To induce colitis, a cohort of mice was treated with 1% DSS, administered in drinking water for 7 days, followed by 5 days of untreated water. These mice showed decreases in body weight of 4% and 9% at days 7 and 11, respectively. Ex vivo pathological

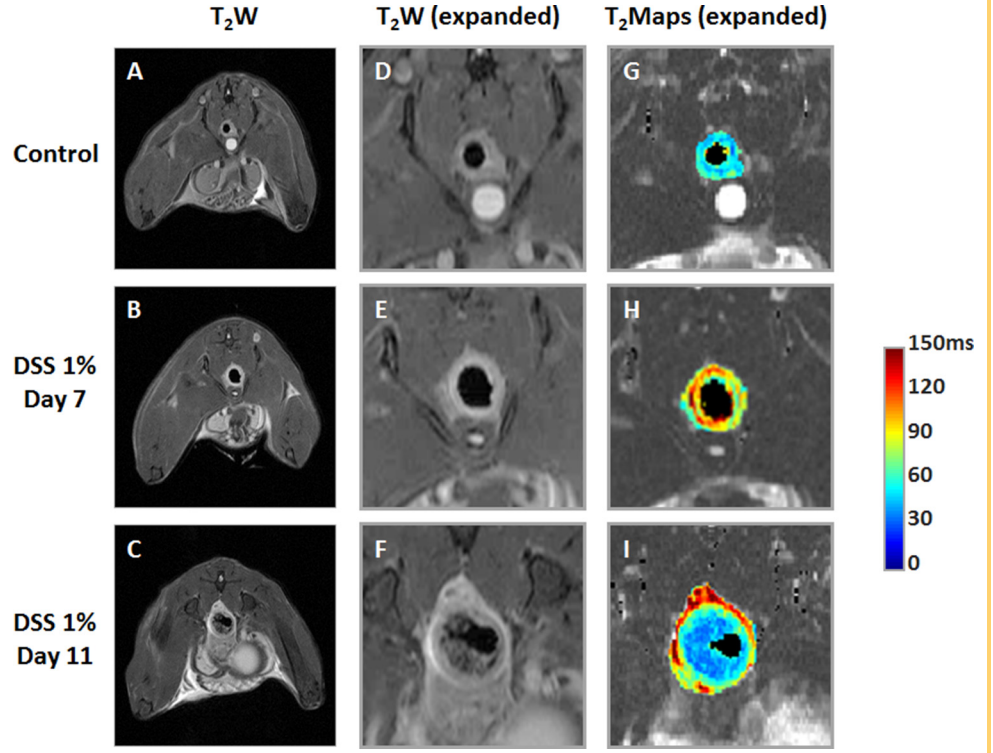

Figure 3. In vivo colon MRI quantification of untreated and treated mice. The T2-weighted (T2W) magnetic resonance (MR) images (A–C), and corresponding expanded regions, showing T2W images (D–F) and T2 maps (G–I), of a representative untreated mouse and a mouse treated with 1% dextran sodium sulfate (DSS), on post-treatment days 7 and 11, respectively.

analysis showed significantly shorter colons, owing to inflammation and edema, in the 1% DSS-treated mice (5.4 ± 0.2 cm) vs untreated controls (7.2 ± 0.4 cm, $P < .0001$).

Figure 3 shows in vivo MRI data from a representative untreated mouse (top row) and a 1% DSS-treated mouse at days 7 (middle row) and 11 (bottom row). Examples of T2-weighted images, both full (Figure 3, A–C) and expanded (Figure 3, D–F) and expanded T2 maps (Figure 3, G–I) are shown. In the T2-weighted MR images, the signal of the colon wall of the 1% DSS-treated mouse at days 7 and 11 is hyperintense compared with that of the untreated mouse. Also, these images reveal a significant change in the colon diameters of the treated mice at day 11. T2 maps show higher T2 values for the DSS-treated colon at days 7 and day 11 (yellow and red pixels) than for the colon of an untreated mouse (blue pixels).

Table 1 shows mean colon T2 values and apparent colon thickness, calculated from the T2 maps, as averages across all image sections. The mean T2 values for colons from the 1% DSS-treated mice were significantly higher on days 7 (83 ± 15 milliseconds) and 11 (88 ± 6 milliseconds) than for colons from untreated mice (61 ± 2 milliseconds, $P < .05$ and $P < .0001$ vs post-DSS-treatment days 7 and 11, respectively). Although no significant change in colon thickness was observed on post-treatment day 7, an increase in the mean apparent colon thickness after 1% DSS treatment was observed at day 11 (0.90 ± 0.07 cm) vs untreated colon (0.51 ± 0.03 cm, $P < .005$).

Table 1. Quantitative Analysis of T2 Maps

	Mean Colon T2 Value [ms]	Mean Apparent Colon Thickness [mm]
Control (n = 6)	61.0 ± 2.0	0.51 ± 0.03
1% DSS—Day 7	83.3 ± 15.4*	0.49 ± 0.06
1% DSS—Day 11	88.3 ± 5.8***	0.90 ± 0.07**

Note: The quantitative analysis allows calculation of mean colon T2 and colon thicknesses, as averages across all sections, in untreated mice (n = 6) and mice treated with 1% DSS on days 7 (n = 5) and 11 (n = 5). Values are mean ± SD. *$P < .05$, **$P < .005$, and ***$P < .0001$, Student 2-tailed t test.

Mean colon T2 values and thicknesses, calculated on a section-by-section basis, are shown in Figure 4. Unlike untreated, control animals, mean T2 values of the colon wall in mice treated with 1% DSS show little positional dependence, at either day 7 or 11. Thus, because of the positional variation seen in controls, *changes* in mean T2 in treated mice are more pronounced in the distal part of the colon than in the proximal part (Figure 4A). For example, increases in mean T2 values in the most proximal imaging section were 22% ± 20% (day 7) and 18% ± 6% (day 11), while corresponding increases in the most distal section were 44% ± 28% (day 7) and 66% ± 10% (day 11), respectively. At day 11, there is a trend toward increased thickness from distal-to-proximal positions within the colon (Figure 4B). Relative to controls, the effect of the DSS treatment on mean apparent colon thickness is more pronounced in the proximal portion of the colon (increase of 93% ± 45% for the most proximal image section) than in the distal portion (62% ± 24%).

Evaluation of Dose-Dependent DSS-Induced Colitis by Endoscopy, Histology, and MRI Colonoscopy

To characterize the dose dependence of DSS-induced colitis, separate cohorts of mice were treated with 0.5%, 1%, 1.5%, or 2% DSS, administered in the drinking water for 7 days, followed by 5 days of untreated water. Mice treated with 1.5% or 2% DSS

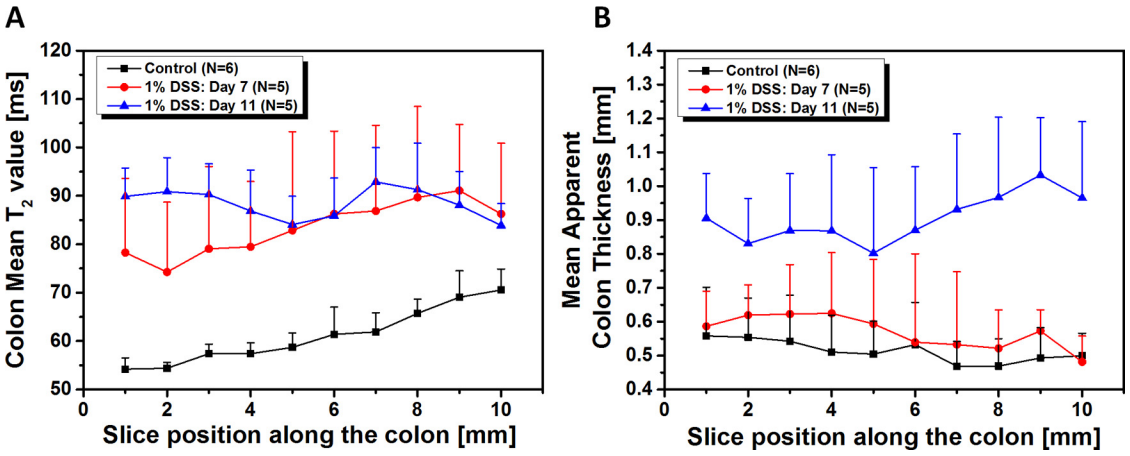

Figure 4. Quantitative analysis of T2 maps calculated from a section-by-section analysis of untreated and treated mice. Mean colon T2 values (A), mean apparent colon thickness as function of section position along the colon in the untreated colon (n = 6), and treated mice with 1% DSS on day 7 (n = 5) and 11 (n = 5) (B). Values are reported as mean ± SD. *$P < .05$ Student 2-tailed *t* test, for all section positions, for both mean colon T2 values, and mean apparent colon thickness, except for the mean colon T2 values at a section position of 7 mm.

showed a decrease in body weight of up to 24% on day 7 and up to 31% on day 11. Ex vivo analysis revealed significantly shorter colons in mice treated with 1%, 1.5%, or 2% DSS-treated mice [average colon lengths, 5.4 ± 0.2 ($P < .00003$), 5.5 ± 1.0 ($P < .004$), and 5.3 ± 1.1 cm ($P < .005$), respectively vs untreated mice (7.2 ± 0.4 cm). No significant differences were observed between the untreated and 0.5% DSS-treated colons (7.2 ± 0.4 cm). Mice treated with 0.5%, 1%, 1.5% or 2% DSS were also characterized, in detail, by endoscopy, histology, and MRI colonoscopy.

As described in Methods/Endoscopy, the endoscopy scoring is based on colon wall thickening, vascularity, presence of fibrin, mucosal granularity, and stool consistency. Each parameter receives a score of 0, 1, 2, or 3, and the composite endoscopy score is the sum of all of the parameter scores. The endoscopy scores for the 0.5%, 1%, 1.5%, and 2% DSS-treated mice were 2.5 ± 0.6, 3.3 ± 1.4, 8.6 ± 1.3, and 10.3 ± 0.6 at day 7, and 4.3 ± 0.8, 10.0 ± 1.2, 10.8 ± 1.3, and 13.7 ± 0.6 at day 11, respectively. *P*-values calculated by comparing these values with endoscopy scores for the untreated groups were all <.001. On both days 7 and 11, endoscopy scores were higher for higher levels of DSS treatment, and scores increased between days 7 and 11 for all treatment groups.

Figure 5A shows representative H&E-stained sections and corresponding endoscopy images of the colon on day 11 for mice treated with 0.5%, 1%, 1.5%, and 2% DSS. Colons of untreated mice had intact mucosa, as shown in Figure 2D. There was neither endoscopic nor microscopic evidence of colitis in the 0.5% DSS group. In colons of the 1%, 1.5%, and 2% DSS groups, there was extensive to diffuse crypt loss and ulceration, accompanied by severe submucosal edema (arrows in Figure 5A) and variable inflammatory infiltration. In the 1.5% and 2% DSS-treated mice, there was free blood in the intestinal lumen (marked with *). As detailed in Methods/Histopathology, mice were scored on a histology scale ranging from 0 (no evidence of inflammation) to 4 (severe inflammation with transmural leukocyte infiltration and loss of goblet cells). The histology scores for the 0.5%, 1%, 1.5%, and 2% DSS-treated mice were 0.2 ± 0.3, 2.1 ± 0.8, 3.1 ± 0.5, and 4.0 ± 0.1, respectively, on day 11. A good correlation was found between the in vivo endoscopy scores and the histology scores (Figure 5B).

Representative T2 maps from mice treated with 0.5%, 1%, 1.5%, or 2% DSS are shown in Figure 6A. The image intensities of the colons of these mice were elevated at both days 7 and 11. The maps of the 0.5% DSS group were similar to those of untreated controls. Mean colon T2 values and apparent colon thicknesses, extracted from the T2 maps and averaged across all imaging sections, are shown in Figure 6B and 6C, respectively. DSS treatment, at levels of 1%–2%, caused significant increases in mean colon T2 values at days 7 and 11, whereas no significant differences were measured at either time point for mice treated with 0.5% DSS. Apparent colon thickness followed a different pattern of response to DSS treatment. On day 7, no significant changes in colon thickness were observed at any level of DSS treatment, whereas on day 11, significant increases ($P < .02$) in wall thickness were observed for mice treated with 1% or greater DSS.

Mean colon T2 values and mean apparent colon thickness parameters were also calculated on a section-by-section basis for each DSS level (Figure 7). For all levels of DSS treatment, section-by-section analysis of apparent colon thickness showed no significant changes on day 7 (Figure 7A). No changes were observed on day 11 for the 0.5% DSS-treated mice. However, at all section positions, there was a significant increase in the mean apparent colon thickness on day 11 for all mice treated with >0.5% DSS (Figure 7B), and a significantly higher mean apparent colon thickness was observed for all mice treated with >0.5% DSS. Somewhat surprisingly, the highest mean apparent colon thickness was found in 1% DSS-treated mice.

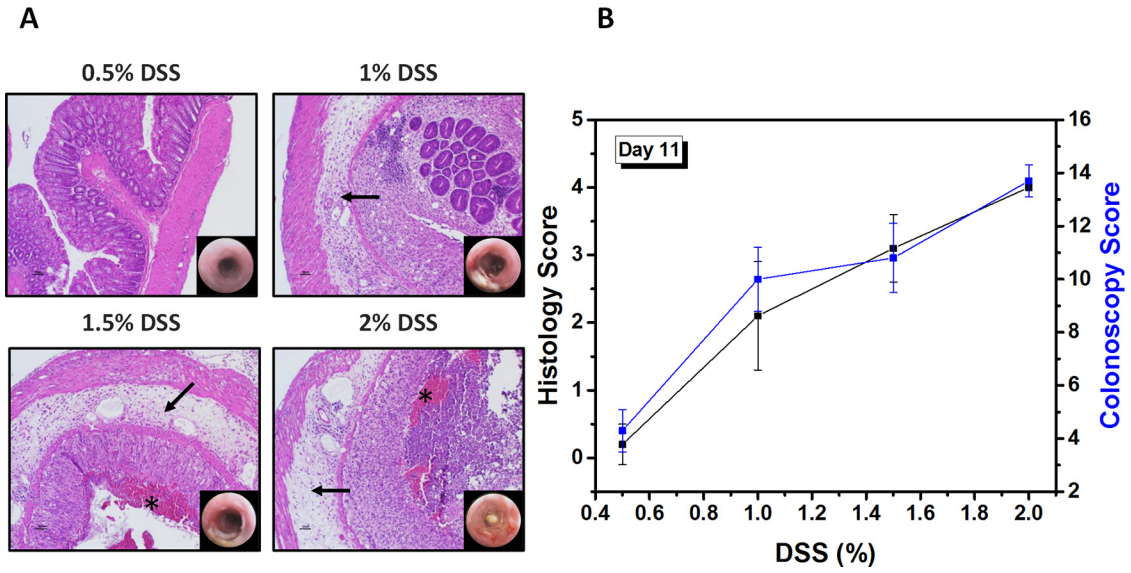

Figure 5. H&E-stained colon sections, and corresponding endoscopy images, taken on day 11, from treated mice with 0.5%–2% DSS (A). Correlation between histology scores and colonoscopy scores as a function of the DSS dose (%). Values are reported as mean ± SD (B).

On day 7, mean colon T2 values for the cohort of 0.5% DSS-treated mice were very similar to those for the untreated group (Figure 7C), with the same trend of increasing T2, proximal to distal, observed in both groups. On day 11, the same proximal-to-distal trend was seen, although a small but significant increase in mean T2 values was observed in the 0.5% DSS-treated mice (Figure 6D). In animals treated with >0.5% DSS, mean colon T2 values increased significantly at all section positions on both day 7 and day 11. The graphs in Figure 7, C–D also show that the effect of DSS treatment (>0.5%) is more pronounced in the distal part of the colon, in particular at day 11.

A Pearson product–moment correlation coefficient was computed to assess the relationship between the MR colonography parameters (average T2 value and colon thickness across all sections) and endoscopy and histology findings at day 11 in the 1% DSS-treated mice. The correlations between average T2 value and measures of endoscopy and histology were significant (Pearson $r = 0.77$ and 0.66, respectively), whereas the corresponding correlations between average colon thickness and these same measures were much weaker (Pearson $r = 0.59$ and 0.50, respectively).

DISCUSSION

UC is a serious and often debilitating condition, with significant long-term consequences for patients. Early detection of UC increases treatment options and improves outcomes, but robust techniques for early detection and accurate monitoring of in vivo treatment response in UC patients are lacking. This study aimed to show the use of a noninvasive MR imaging technique, T2 mapping, for identifying and quantitatively grading UC in a chemically induced mouse model. We showed clearly that our T2-based MR experiments and analysis can provide a quantitative measure of UC inflammation on a positional (ie, section-by-section) basis along the colon. Our MRI findings were validated by endoscopic evaluation and colon biopsies. The quantitative information about colitis activity and colon wall thickness derived from noninvasive MR experiments can be readily translated to the clinic for improved early detection of UC and monitoring of the efficacy of treatment in UC patients.

As noted earlier, MRI-derived metrics, including measures of colon wall thickness and inflammation and gadolinium (contrast-agent) enhancement, have established MRI as an important, noninvasive imaging modality for detecting morphologic changes and inflammatory activity associated with IBD. However, these findings are consistently observed in only severe and active UC. In moderate and quiescent stages of UC disease, no effect on the colon wall thickness is found (15), and current MRI methods are not sensitive enough for robust detection of UC. Herein, we show quantitative T2 mapping, including both positional dependence and average along the colon, as a method for improving evaluation of the extent and severity of UC, thereby improving early, accurate diagnosis.

Our initial experiments focused on the characterization of healthy, untreated colon. As expected, no significant differences were found in the mean colon wall thickness along the length of the colon. Somewhat surprisingly, T2 mapping revealed higher T2 values in proximal vs distal regions, findings that correlated with positionally dependent differences in tissue architecture and cellular composition. These findings were mirrored in differences observed histologically. The mouse basic bowel wall structure includes the mucosa, submucosa, muscularis, and serosa. The mouse muscularis propria has inner circular and outer longitudinal layers. The mouse cecal muscular layers are thinner than the more distal colon muscular layers. The muscular tunics increase in thickness progressively in the distal and

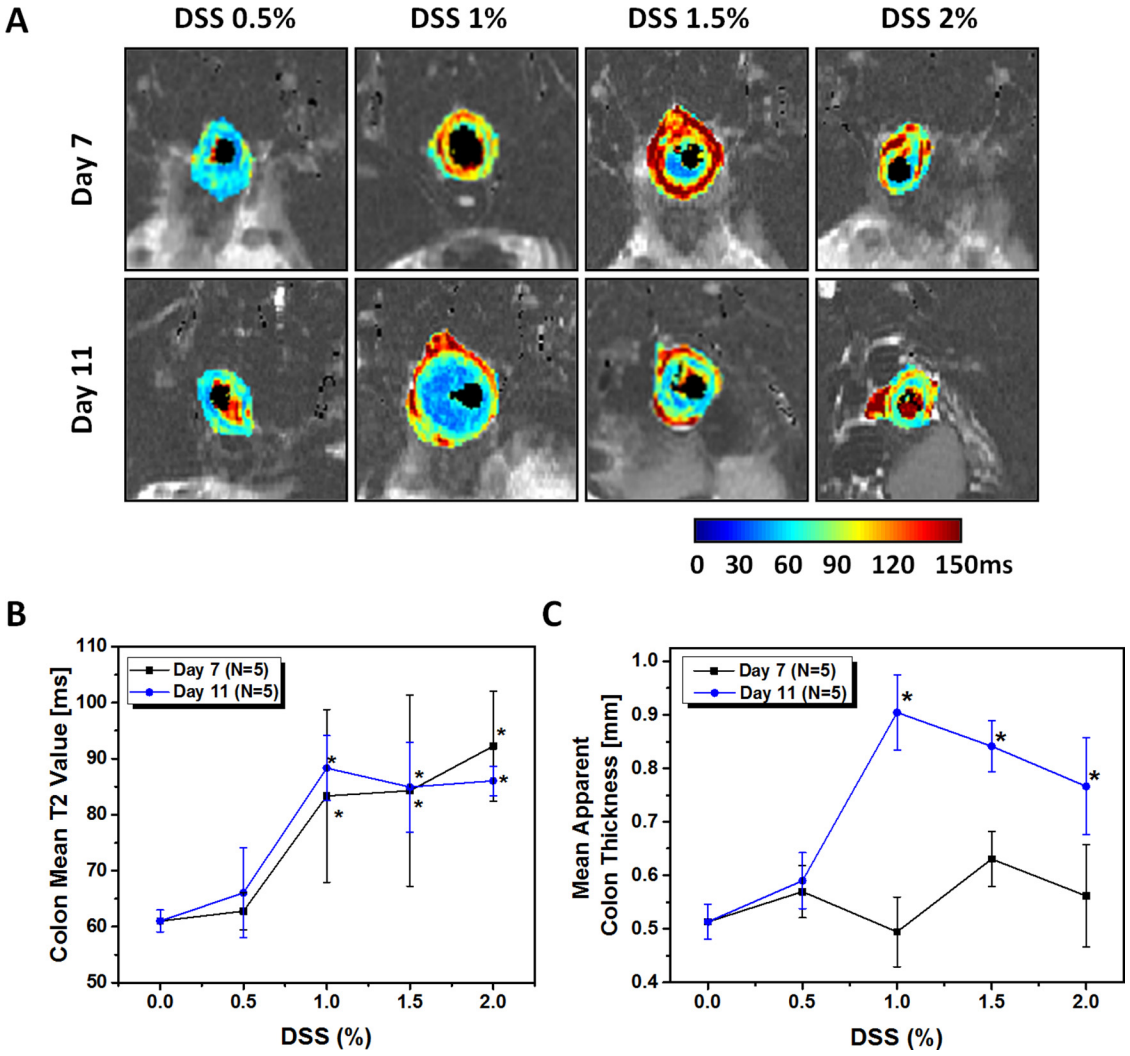

Figure 6. DSS dosage response. The T2 maps of representative treated mice with different DSS ratio from 0.5% to 2% on day 7 and 11 (A). Quantitative analysis of T2 maps, as an average value across all sections of untreated and treated mice, at different DSS ratios. Mean colon T2 values (B), Mean apparent colon thickness in untreated (0% DSS) colon (n = 6), and treated mice with 0.5%–2% DSS on day 7 (n = 5) and 11 (n = 5) (C). Values are reported as mean ± SD. *$P < .05$ Student 2-tailed *t* test.

descending colon. The mucosa of mouse proximal colon has transverse folds that are longer than those present in the cecum. Mouse midcolonic mucosa is flat with no mucosal folds. The distal colon of the mouse has longitudinal mucosal folds.

In UC in human, ulcers gradually spread upward from their points of origin, until the entire colon is involved. Thus, a method that can improve diagnostic sensitivity on a positional basis has direct translational importance. Our MRI-derived metrics, which showed sensitivity to positionally dependent colon thickening and inflammation, may have clinical relevance to the diagnosis of UC, in particular at early stages of the disease.

One of the significant differences between this work and earlier studies is the examination of the effects of lower levels of DSS treatment. Although most previous experiments were performed with high dosage (≥2% wt/vol) of DSS in the drinking water (7-9, 20), here, we examined mice treated with as little as 0.5% DSS. The development of imaging markers in these lower-dosage studies has potential importance for the early-stage diagnosis of IBD. Below 1% DSS, our T2-based, MR colonography tool was unable to detect changes in the colon, an observation that was consistent with colonoscopy and, in particular, histology in these same mice. However, in 1% DSS-treated animals, the in vivo MRI-grading tool revealed significant inflammation at post-treatment days 7 and 11, as reflected by increases in mean colon T2 of 36% and 45%, respectively. Section-by-section analysis of T2 maps showed that the inflammation was positionally dependent along the colon, being more pronounced distally than proximally. This finding is consistent with a report by Suzuki et al., that the severity of inflammation, measured by histology, was the greatest in the distal region of the colon in a DSS colitis mouse model initiated with azoxymethane (24).

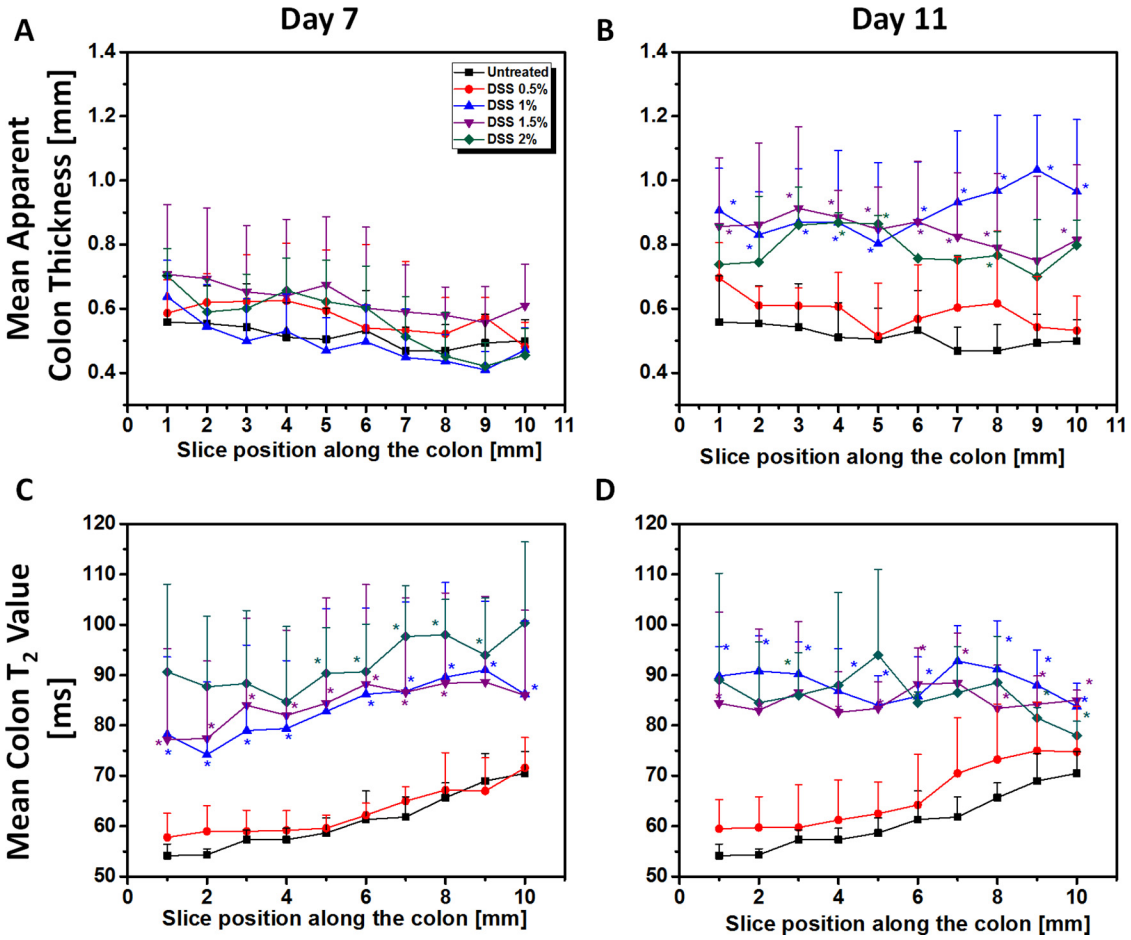

Figure 7. Quantitative analysis of T2 maps calculated from a section-by-section analysis of untreated and treated mice at different DSS ratio. Mean apparent colon thickness values in untreated (0% DSS) colon (n = 6) and treated mice with 0.5%–2% DSS on day 7 (A) (n = 5) and 11 (B) (n = 5). Mean colon T2 values in untreated (0% DSS) colon (n = 6) and treated mice with 0.5%–2% DSS on day 7 (C) (n = 5) and 11 (D) (n = 5). Values are reported as mean ± SD.

Of note, MRI-derived colon wall thickness was unaffected at post-treatment day 7 following 1% DSS administration. Thus, T2 mapping proved more sensitive to early DSS-induced pathology than wall thickness. By post-treatment day 11, the colon wall thickness was increased, with greater thickening of the wall in the proximal portion of the colon than in the distal portion.

In the current study, colonoscopy and histology scores at post-treatment day 11 increased with increasing DSS dose (above 0.5% DSS). MRI findings at days 7 and 11 provided important insights into the dose dependence of DSS-induced injury. Based upon observed increases in T2, DSS dose-dependent colonic inflammation was similar at days 7 and 11 for all DSS levels >0.5%, and showed little positional dependence along the colon. However, compared with T2 values for normal colon, T2 increases for DSS levels >0.5% were greater in the distal region of the colon.

A different pattern was observed for MRI-derived colon wall thickness as a function of DSS level. At post-treatment day 7, colon wall thickness for all DSS levels was similar to normal colon, and was positionally independent. By contrast, at day 11, significant increases in colon wall thicknesses were observed for DSS levels >0.5%. Again, no positional dependence of wall thickness was observed. Interestingly, the greatest increase in the colon wall thickness at day 11 was observed for mice treated with 1% DSS. In total, our MRI results suggest that treating mice with 1% DSS in drinking water for 7 days, followed by 5 days of regular water, produces the most severe colitis, with better reproducibility and lower mortality than higher doses of DSS.

The use of sensitive T2 mapping-based MR colonography, together with improved reproducibility and lower mortality of the murine 1% DSS-induced colitis model, will provide new opportunities for studying therapeutic drugs to combat the disease. MR imaging will allow longitudinal monitoring of therapeutic response and improve sensitivity for detecting healing at specific locations along the colon.

In summary, findings from the present study suggest that the established, T2 mapping-based MR colonography tool can be used to reliably characterize colon damage in a chemically induced mouse model. It was demonstrated clearly that colon

thickness, measured via conventional, T2-weighted sequences, is insufficient for assessing disease severity, in particular, in the early stages. Mean T2 value, an MR biomarker of inflammation, was found to be quantitative and sensitive to disease severity.

ACKNOWLEDGMENTS

We thank Dr. Scott Beeman, Washington University, for stimulating conversations and for his careful reading of this manuscript.

Disclosures: No disclosures to report.

Conflict of Interest: The authors have no conflict of interest to declare.

REFERENCES

1. Torres MI, Rios A. Current view of the immunopathogenesis in inflammatory bowel disease and its implications for therapy. World J Gastroenterol. 2008;14: 1972–1980.
2. Kaplan GG. The global burden of IBD: from 2015 to 2025. Nat Rev Gastroenterol Hepatol. 2015;12:720–727.
3. Ng SC, Shi HY, Hamidi N, Underwood FE, Tang W, Benchimol EI, Panaccione R, Ghosh S, Wu JCY, Chan FKL, Sung JJY, Kaplan GG. Worldwide incidence and prevalence of inflammatory bowel disease in the 21st century: a systematic review of population-based studies. Lancet. 2018;390(10114):2769–2778 [Epub 2017].
4. Randhawa PK, Singh K, Singh N, Jaggi AS. A review on chemical-induced inflammatory bowel disease models in rodents. Korean J Physiol Pharmacol. 2014; 18:279–288.
5. Larsson AE, Melgar S, Rehnstrom E, Michaelsson E, Svensson L, Hockings P, Olsson LE. Magnetic resonance imaging of experimental mouse colitis and association with inflammatory activity. Inflamm Bowel Dis. 2006;12:478–485.
6. Wirtz S, Neurath MF. Mouse models of inflammatory bowel disease. Adv Drug Deliv Rev. 2007;59:1073–1083.
7. Wirtz S, Neufert C, Weigmann B, Neurath MF. Chemically induced mouse models of intestinal inflammation. Nat Protoc. 2007;2:541–546.
8. Mustafi D, Fan X, Dougherty U, Bissonnette M, Karczmar GS, Oto A, Hart J, Markiewicz E, Zamora M. High-resolution magnetic resonance colonography and dynamic contrast-enhanced magnetic resonance imaging in a murine model of colitis. Magn Reson Med. 2010;63:922–929.
9. Beltzer A, Kaulisch T, Bluhmki T, Schoenberger T, Stierstorfer B, Stiller D. Evaluation of quantitative imaging biomarkers in the DSS colitis model. Mol Imaging Biol. 2016;18:697–704.
10. Hommes DW, van Deventer SJ. Endoscopy in inflammatory bowel diseases. Gastroenterology. 2004;126:1561–1573.
11. Eliakim R, Magro F. Imaging techniques in IBD and their role in follow-up and surveillance. Nat Rev Gastroenterol Hepatol. 2014;11:722–736.
12. Slovak JE, Wang C, Sun Y, Otoni C, Morrison J, Deitz K, LeVine D, Jergens AE. Development and validation of an endoscopic activity score for canine inflammatory bowel disease. Vet J. 2015;203:290–295.
13. Ajaj WM, Lauenstein TC, Pelster G, Gerken G, Ruehm SG, Debatin JF, Goehde SC. Magnetic resonance colonography for the detection of inflammatory diseases of the large bowel: quantifying the inflammatory activity. Gut. 2005;54:257–263.
14. Laghi A, Borrelli O, Paolantonio P, Dito L, Buena de Mesquita M, Falconieri P, Passariello R, Cucchiara S. Contrast enhanced magnetic resonance imaging of the terminal ileum in children with Crohn's disease. Gut. 2003;52:393–397.
15. Maccioni F, Colaiacomo MC, Parlanti S. Ulcerative colitis: value of MR imaging. Abdom Imaging. 2005;30:584–592.
16. Pupillo VA, Di Cesare E, Frieri G, Limbucci N, Tanga M, Masciocchi C. Assessment of inflammatory activity in Crohn's disease by means of dynamic contrast-enhanced MRI. Radiol Med. 2007;112:798–809. [Article in English, Italian]
17. Zimmermann EM, Al-Hawary MM. MRI of the small bowel in patients with Crohn's disease. Curr Opin Gastroenterol. 2011;27:132–138.
18. Adler J, Swanson SD, Schmiedlin-Ren P, Higgins PD, Golembeski CP, Polydorides AD, McKenna BJ, Hussain HK, Verrot TM, Zimmermann EM. Magnetization transfer helps detect intestinal fibrosis in an animal model of Crohn disease. Radiology. 2011;259:127–135.
19. Breynaert C, Dresselaers T, Perrier C, Arijs I, Cremer J, Van Lommel L, Van Steen K, Ferrante M, Schuit F, Vermeire S, Rutgeerts P, Himmelreich U, Ceuppens JL, Geboes K, Van Assche G. Unique gene expression and MR T2 relaxometry patterns define chronic murine dextran sodium sulphate colitis as a model for connective tissue changes in human Crohn's disease. PloS One. 2013;8: e68876.
20. Melgar S, Gillberg PG, Hockings PD, Olsson LE. High-throughput magnetic resonance imaging in murine colonic inflammation. Biochem Biophys Res Commun. 2007;355:1102–1107.
21. Walldorf J, Hermann M, Porzner M, Pohl S, Metz H, Mader K, Zipprich A, Christ B, Seufferlein T. In-vivo monitoring of acute DSS-colitis using colonoscopy, high resolution ultrasound and bench-top magnetic resonance imaging in mice. Eur Radiol. 2015;25:2984–2991.
22. Becker C, Fantini MC, Neurath MF. High resolution colonoscopy in live mice. Nat Protoc. 2006;1:2900–2904.
23. Navarro M, Ruberte J, Carretero A, Nacher V, Dominguez E. Digestive Tract. In: Ruberte J, Carretero A, Navarro M, editors. Morphological Mouse Phenotyping: Anatomy, Histology and Imaging: Academic Press; 2017;89–146.
24. Suzuki R, Kohno H, Sugie S, Tanaka T. Dose-dependent promoting effect of dextran sodium sulfate on mouse colon carcinogenesis initiated with azoxymethane. Histol Histopathol. 2005;20:483–492.